NIH Public Access
Author Manuscript
Circ Res. Author manuscript; available in PMC 2008 February 13.

Published in final edited form as:
Circ Res. 2003 June 13; 92(11): 1209–1216.

Impulse Propagation in Synthetic Strands of Neonatal Cardiac Myocytes With Genetically Reduced Levels of Connexin43

Stuart P. Thomas, **Jan P. Kucera**, **Lilly Bircher-Lehmann**, **Yoram Rudy**, **Jeffrey E. Saffitz**, and **André G. Kléber**

From the Department of Physiology (S.P.T., L.B.-L., A.G.K.), University of Bern, Switzerland; the Center for Cardiovascular Research and the Department of Pathology (J.E.S.), Washington University, St. Louis, Miss; and the Department of Biomedical Engineering (J.P.K., Y.R.), Case Western Reserve University, Cleveland, Ohio.

Abstract

Connexin43 (Cx43) is a major determinant of the electrical properties of the myocardium. Closure of gap junctions causes rapid slowing of propagation velocity (θ), but the precise effect of a reduction in Cx43 levels due to genetic manipulation has only partially been clarified. In this study, morphological and electrical properties of synthetic strands of cultured neonatal ventricular myocytes from $Cx43^{+/+}$ (wild type, WT) and $Cx^{+/-}$ (heterozygote, HZ) mice were compared. Quantitative immunofluorescence analysis of Cx43 demonstrated a 43% reduction of Cx43 expression in the HZ versus WT mice. Cell dimensions, connectivity, and alignment were independent of genotype. Measurement of electrical properties by microelectrodes and optical mapping showed no differences in action potential amplitude or minimum diastolic potential between WT and HZ. However, maximal upstroke velocity of the transmembrane action potential, dV/dt_{max}, was increased and action potential duration was reduced in HZ versus WT. θ was similar in the two genotypes. Computer simulation of propagation and dV/dt_{max} showed a relatively small dependence of θ on gap junction coupling, thus explaining the lack of observed differences in θ between WT and HZ. Importantly, the simulations suggested that the difference in dV/dt_{max} is due to an upregulation of I_{Na} in HZ versus WT. Thus, heterozygote-null mutation of Cx43 produces a complex electrical phenotype in synthetic strands that is characterized by both changes in ion channel function and cell-to-cell coupling. The lack of changes in θ in this tissue is explained by the dominating role of myoplasmic resistance and the compensatory increase of dV/dt_{max}.

Keywords

synthetic cardiac strands; neonatal mouse cardiomyocytes; connexin43 expression; conduction velocity

Propagation of the cardiac impulse is a complex process that depends on the active electrical properties of myocyte membranes and the passive properties of the cellular network. The connexin proteins form the electrical connections between myocytes, and are therefore important determinants of the myocardial electrical properties. The most abundant connexin in ventricular myocardium of both mice and humans is connexin43 (Cx43).[1] The overall electrical conductance between cardiac cells can be changed in two basic ways: (1) by affecting gap junctional conductance (drugs[2,3] and myocardial ischemia[4]), or (2) by changing connexin expression.[5] Computer simulations[6] and experimental studies[7] have shown that a large reduction in gap junctional conductance can result in reduction of θ to values of a few

Correspondence to André G. Kléber, MD, Department of Physiology, University of Bern, Bühlplatz5, CH-3012 Bern, Switzerland. E-mail kleber@pyl.unibe.ch.

NIH-PA Author Manuscript
NIH-PA Author Manuscript
NIH-PA Author Manuscript

NIH-PA Author Manuscript

NIH-PA Author Manuscript

NIH-PA Author Manuscript

centimeters per second, an extreme degree of slowing that cannot be achieved with suppression of current flow through ion channels.[8] More moderate changes in gap junctional conductance due to a change of connexin expression have been shown to occur in ventricular hypertrophy and failure[9,10] and after application of mediators of hypertrophy[11] and mechanical stretch.[12]

Mice with a targeted deletion of Cx43 have reduced expression of this protein in vivo.[13] Cx43-null mice ($Cx43^{+/-}$) have major cardiac abnormalities and die soon after birth.[14,15] Heterozygotes ($Cx43^{-/-}$, HZ) have a normal macroscopic cardiac morphology, an approximately 50% decrease in Cx43 expression,[16–20] survive, and are able to breed. No differences in active membrane properties between HZ and wild-type (WT) littermates have been observed in cells isolated from adult mice.[17] However, a difference in occurrence of arrhythmias during acute myocardial ischemia indicated at least concealed differences in function between WT and HZ.[21] Propagation velocity, θ, in HZ mice was measured in intact ventricle with conflicting results. Three studies revealed a significantly lower average θ and a widening of the QRS complex in HZ versus WT mice,[16,17,19] and two studies showed no changes in θ.[18,20] An indication that the relationship between genetic manipulation of Cx43 expression and conduction velocity change might be complex was also given by observations in conditional knockout (CKO) mice with marked, heart-specific deletion of Cx43. These mice had an increased incidence of arrhythmias and sudden death only 2 months after birth, and showed no previous major signs of mechanical or electrical dysfunction, despite the marked changes in cell-to-cell connections.[22]

The aim of the present study was to study the changes in connexin expression in HZ versus WT mice with Cx43 deletion, and the consequences of such deletion for electrical function in synthetic murine myocyte strands at the cellular level of resolution. In such a way, several parameters, which might affect conduction velocity, could be measured and introduced into a computer model to elucidate the complex functional relationships among the experimentally determined parameters.

Materials and Methods

Cell Cultures

The technique used for patterned growth of neonatal mouse ventricular myocytes has previously been described.[23] The genotypes of all mice were determined by polymerase chain reaction using protocols modified from those of Reaume et al.[14] The cell suspensions were then preplated to eliminate fibroblasts and seeded on prepared coverslips to produce patterned growth. Myocytes were grown in 1-cm-long growth channels of 3 widths (100, 80, and 60 μm) as a dense continuous monolayer of anisotropically arranged cells.[23,24] A total of 114 mice were used for 14 culture preparations. In addition, control experiments assessing Cx45 immunofluorescence were made in cultures from mice hearts (Jackson Labs, Bar Harbor, Maine) excised at embryonic day 20 (E20). The study complied with the ethical principles described by the Swiss Academy of Medical Science and institutional guidelines were observed.

Electrophysiological Measurements and Analysis of Propagation

The technique of multiple site optical recording of transmembrane potential, the staining of cell cultures with the voltage-sensitive dye RH237, the construction of isochronal maps, and the determination of θ have been described in detail elsewhere.[23–25] For measurement of both individual action potentials and θ, the cultures were stimulated >1 mm from the recording site within a strand (cycle length 500 ms, rectangular pulse of 5 ms duration).

NIH-PA Author Manuscript

NIH-PA Author Manuscript

NIH-PA Author Manuscript

Microelectrode measurements were performed to calibrate the action potential amplitude of the optical recordings and to measure action potentials as described previously.[23]

Immunohistochemistry and Confocal Microscopy

Fixation of cultures and immunostaining for Cx43 and Cx45, including all immunostaining procedures, such as controls for nonspecific binding, have been described in detail in previous reports.[13,23,26] Also, the details of the morphological analysis to determine cell size, cell length, and angle of alignment have been published previously.[23,24,27]

Computer Simulation of Propagation and the Mean Maximal Upstroke Velocity of the Transmembrane Action Potential, dV/dt_{max}

The process of cardiac impulse propagation was simulated in chains of 181 cells in length, using the modification of the Luo-Rudy model cells described by Faber.[28,29] First, propagation was simulated to match the results (θ and dV/dt_{max}) of the WT mice by adapting gap junctional conductance and the maximal conductance of the Na^+ current. Subsequently, a match was made to the values observed in HZ mice. Whereas the surface-to-volume ratio of the cylindrical model cell was left unchanged, the cells were reduced in size to a length of 40 μm and a diameter of 10 μm. For WT and HZ mice, a fit to the experimental values was obtained with a cytoplasmic resistivity of 124 Ωcm, which is close to experimentally determined values.[30]

Statistical Analysis

The Student's *t* test was used for morphological comparisons between the two genotypes. The Student's *t* test and multiple regression were used to determine the effect of genotype on dV/dt_{max} and θ. Significances between multiple groups were determined using ANOVA. Continuous variables are expressed as mean ± SD.

An expanded Materials and Methods section can be found in the online data supplement available at http://www.circresaha.org.

Results

Cell Dimensions

Computer simulations have recently demonstrated that cell dimensions are important parameters affecting velocity and the shape of the action potential during propagation.[31] Therefore, cell length, cell width, angle of cell alignment, and connectivity were determined in growth channels of different widths in both WT and HZ mice. The morphometric parameters were all closely similar to wild-type synthetic mice strands with a different genetic background (ddY mice).[23] Average cell width in WT 80-μm strands was 13.8 ± 1.9 μm, and average cell length was 35.7 ± 4.0 μm (42% of the length and 99% of the width of adult murine WT ventricular cardiomyocytes). There were no statistically significant differences between WT and HZ myocytes.

An expanded Cell Dimensions section can be found in the online data supplement available at http://www.circresaha.org.

Expression of Connexin43 in HZ Versus WT Synthetic Myocyte Strands

Cx43 immunoreactive signal in mouse myocytes in strands was analyzed by quantitative confocal microscopy. Figure 1 shows representative confocal images of immunostained strands from WT and HZ mice. In all cases, the Cx43 signal appeared as discrete spots of high-intensity signal distributed regularly around the cell perimeter. This pattern is identical to the pattern

NIH-PA Author Manuscript

NIH-PA Author Manuscript

NIH-PA Author Manuscript

from synthetic mice strands of "ddY" genetic background and from rat synthetic strands.[23] Table 1 shows the results of quantitative analysis of the amount of Cx43 immunoreactive signal. There was a consistent difference in Cx43 expression in all experiments. Fluorescent labeling of Cx43 was 43% lower in HZ than in littermate WT. This reduction in expression of Cx43 was due to a reduction in gap junction numbers. The mean size of individual gap junctions was unchanged. Moreover, expression of Cx43 was independent of strand width in both genotypes. Control experiments in synthetic strands assessing Cx45 fluorescence at E20 revealed a significant 58% ($P < 0.01$) decrease in HZ (0.39% cell area, n = 12) versus WT (0.75% cell area, n = 9). This is in close accordance with recent Cx45 determinations in adult animals.[26]

Electrical Properties of Synthetic Cardiac Myocyte Strands

An isochronal map constructed from optical recordings of the transmembrane potential upstrokes obtained from a culture of HZ mouse myocytes is shown in Figure 2. In this particular experiment, longitudinal θ along a 60-μm wide strand was 52 cm/s. Statistical analysis of θ obtained from isochronal maps in both genotypes demonstrated no significant differences between the WT and HZ genotypes. Thus, θ was 46.6 ± 13cm/s in the WT group (n = 79, different strands) and 45.0 ± 12cm/s in the HZ group (n = 104, different strands). The confidence intervals of 2.9 cm/s (WT) and 2.2 cm/s (HZ) indicated that differences in θ of > 6 cm/s would be detectable with this method. In contrast to this finding, the upstroke velocity of the optically recorded transmembrane action potential (dV/dt_{max}) was significantly higher in the heterozygote group (173 ± 28% APA/s versus 157 ± 27% APA/s/s; $P < 0.0005$, Table 2).

Microelectrode measurements of transmembrane action potentials (Figure 3) were performed to compare the action potential amplitude between HZ and WT cultures and to assess the time course of repolarization. This comparison was necessary for the interpretation of optical recordings of dV/dt_{max} because the fluorescence change of voltage-sensitive dyes yields only a relative change in transmembrane voltage.[32] The measurements obtained with microelectrode recordings are shown in Table 2. Action potential amplitude and minimum diastolic potential were independent of genotype, and close to 100 mV and −70 mV, respectively. This is very close to values from ddY-WT mice and to rat synthetic strands.[23, 24] In accordance with the optical recordings, the dV/dt_{max} in the heterozygote group was 14% higher than that of the wild-type mice. In contrast to the optical measurements, this difference was not statistically significant, probably because of the small number. The difference in action potential duration illustrated in Figure 3 was due to a relative shortening of the late phase of repolarization (APD 90%; see Table 2) in the HZ strands.

Computer Simulation of Propagation

Propagation is a complex process involving a number of interdependent variables such as cell size and dimension, cell-to-cell coupling, and flow through ion channels. Therefore, computer simulations were performed to assess the relative contributions of these variables to θ and dV/dt_{max}.

Comparison of the changes in dV/dt_{max} as a function of θ is shown in Figure 4. Each point on the "dV/dt_{max} versus θ '" plane corresponds to a given combination of a maximal I_{Na} conductance value with a lumped resistance value of the intracellular space, r_{lumped}, whereby r_{lumped} corresponds to the series resistance per unit length formed by the myoplasmic and junctional resistances ($r_{lumped} = r_{myoplasmic} + r_{junctional}$). For the observed fit with the experimental mean values in WT mice, the r_{lumped} of 2030×10^3 Ω/cm was composed of 78% $r_{myoplasmic}$ and 22% $r_{junctional}$. To calculate the effect of the measured effect of a 43% reduction in gap junction expression in HZ mice, it was first assumed that the reduction in expression was followed by a corresponding increase in $r_{junctional}$. Because of the relatively large

NIH-PA Author Manuscript

NIH-PA Author Manuscript

NIH-PA Author Manuscript

contribution of the $r_{myoplasmic}$, r_{lumped} increased by only 16%, from 203×10^3 to 235×10^3 Ω/cm. At a constant contribution of I_{Na}, this produced a relatively small reduction in θ, from 46.6 to 43.2 cm/s. Thus, the decrease in θ, even in absence of any change in dV/dt_{max}, was below 4 cm/s and would probably not have been detected by our method. Because the morphometric analysis showed an almost 2-fold increase of cell length in adult versus neonatal myocytes, we computed the effect of changing cell length, l, on conduction velocity at a given value of junctional resistance. Increasing l not only increased, as expected, conduction velocity but it also minimized the effect of reduction in gap junction expression on θ, as illustrated on Figure 4B.

The simulated increase of dV/dt_{max} caused by the increase in r_{lumped} was negligible. The fit to the experimentally observed values of dV/dt_{max} in HZ mice required a 12% increase of I_{Na} in the simulations (Figure 4B).

Discussion

As major findings, this work shows that (1) neonatal mice cardiomyocytes with heterozygote null mutation of Cx43 have an average reduction of 43% in expressed levels of Cx43 gap junction protein, (2) the reduction in Cx43 is not followed by a significant reduction in θ, and (3) the significant increase in dV/dt_{max} of the upstroke of the transmembrane action potential suggests an upregulation of I_{Na}.

Reduction in Cx43 Protein in Synthetic Strands of Genetically Modified Mice and Reduction in Cell Size

Previous comparison of changes in immunofluorescence of Cx43 with electron-microscopic measurements of gap junction size and numbers have shown a close correlation, suggesting that immunofluorescence analysis in ventricular myocytes provides a reliable measure of connexin43 location in gap junctions and the number and relative size of these junctions.[13] Moreover, all studies performed with mice harboring a null mutation of the Cx43 gene have suggested a reduction of connexin expression and/or in electrical cell-to-cell coupling.[16–18,22,33] Immunohisto-chemical staining of Cx43 located in the gap junctions in the adult mouse heart has shown a reduction of Cx43 expression by 45%,[16] a value closely similar to the 43% reduction in our synthetic strands. Also, the absolute values of Cx43 signal were similar in both studies. These observations show that there is no difference between neonatal and adult myocytes in the reduction of Cx43 expression caused by a null allele. In control experiments, we assessed coexpression of connexin 45 (Cx45) in WT and HZ animals. In accordance with results in adult mice,[26] there was a significant concomitant decrease in Cx45 immunofluorescence in HZ versus WT animals. As a consequence, an upregulation of Cx45 in the HZ Cx43 animals can be excluded as a compensatory mechanism to maintain intercellular communication.

Relation Between Cx43 Reduction, Cell-to-Cell Coupling, and Changes in Propagation Velocity

Propagation velocity measurements in HZ Cx43 mice performed with optical mapping have shown variable results. Thus, the absolute θ values in the longitudinal direction of the cardiac fiber axes in mice were approximately 30 cm/s in the first study[17] (measured at 31°C), whereas they amounted to ≥55 cm/s in further studies.[16,18] Moreover, two of these studies showed a decrease of θ in the HZ group,[16,17] whereas another study did not detect any difference in θ between the WT and the HZ hearts.[18] Also, measurements of θ in embryonic hearts failed to detect a difference between HZ and WT animals.[20] A recent study measuring θ in mice with cardiac-specific homozygote conditional knockout (CKO) mice ($Cx43^{-/-}$) showed that an almost complete absence of Cx43 (reduction to 5% of normal) was accompanied by normal

NIH-PA Author Manuscript

NIH-PA Author Manuscript

NIH-PA Author Manuscript

mechanical heart function immediately after birth with only a ≈ 50% decrease in longitudinal θ.[22]

In the present study performed with optical mapping techniques at the cellular level, some problems related to θ measurements in whole hearts, such as virtual electrode effects[34] during point stimulation and curvature effects,[35] were avoided. The high sampling rate (< 50 μs) and high spatial resolution (15 μm) enabled the measurement of the action potential upstroke with high accuracy.[25] Our findings of no difference in θ between the WT and the HZ groups are in accordance with the results of Morley et al[18] and Vaidya et al[20] but contrast to the measurements of Guerrero et al[17] and Eloff et al.[16] It is possible that the controversial results in the measurements of θ observed in whole mice hearts may relate to some of the methodological difficulties discussed,[16] which were avoided with our technique.

The simulations took account of the cell dimensions observed in neonatal mice and assumed that the decrease in immunofluorescence observed in the HZ group was followed by a corresponding decrease in cell-to-cell conductance. A fit to both dV/dt_{max} and θ in the WT and the HZ group was obtained with the assumption of a myoplasmic resistivity of $R_{myoplasmic}$ = 124 Ωcm, a value that was well in the range of experimental measurements in rabbit ventricular myocardium.[30] As a first result, the simulation study showed that a 43% decrease in cell-to-cell coupling alone leads to a small increase of 16% in the lumped intracellular resistance and to a concomitant decrease of conduction velocity by only 7%. This is at the limit of detection with high-resolution optical mapping. This very small dependence of θ on the change in connexin expression can be explained by the fact that r_{lumped}, which corresponds to the sum of $r_{myoplasmic}$ and $r_{junctional}$, was mainly determined by $r_{myoplasmic}$. Interestingly, our simulation studies also suggest that the seeming discrepancy between the marked reduction in Cx43 expression (average 95%) and the moderate reduction in θ (50%)[22] in CKO mice may in fact be due to the relatively large contribution of $r_{myoplasmic}$ to θ. Although the nonhomogenous distribution of residual Cx43 in the CKO mice differs from the homogenous arrangement of $r_{junctional}$ in our model, computation using our model yields a very similar result (55% decrease in θ for a 95% decrease in cell-to-cell coupling).

A recent simulation of continuous and discontinuous propagation at a cellular level has shown that cell length, in addition to the pattern of gap junction distribution, is a major determinant of θ.[31] In the case of continuous conduction, this dependence is due to the increase in density of gap junctions along the axis of propagation with decreasing cell length. The dependence of the relationship between gap junction expression and θ on cell length, as shown on Figure 4B, may explain the observation that longitudinal θ in the normal adult mouse heart is faster (between 58 and 67 cm/s[16,22]) than in the synthetic murine strands. Thus, measurements taken from histological sections of adult hearts of either genotype revealed that the cell length of adult mice is about twice the average length of the neonatal myocytes in the narrow synthetic strands. Inversely, theory predicts that the difference in θ between WT and HZ mice decrease with increasing cell length and conduction velocity, because the gap junctional resistance contributes less to r_{lumped} per unit length.

In recent studies, a change in θ was consistently observed in isotropic rat myocyte cultures on application of dibutyryl cAMP,[11] acute pulsatile stretch,[12] and vascular endothelial growth factor.[36] The calculated close correlation between the changes in gap junction expression and in θ in those studies was based on computations in linear cell strands[8] and experiments in rats,[25] showing that about 50% of the conduction delay is located at the gap junction and 50% in the cytoplasm. These studies and the present work underline the importance of the relative contributions of gap junctional resistance and cytoplasmic resistance to the process of propagation, which may vary among species. Moreover, they suggest that the change in gap

NIH-PA Author Manuscript

NIH-PA Author Manuscript

NIH-PA Author Manuscript

junction expression in the studies performed with rat neonatal myocyte cultures and in the present study are followed by a proportional change in average $r_{junctional}$.

The Shape of the Transmembrane Action Potential and Changes in Cell-to-Cell Coupling

The dependence of the shape of the transmembrane action potential upstroke on propagation is related to the discontinuous nature of the cardiac propagation process, and therefore, is expected to vary with the degree of discontinuity. During propagation in simulated cell chains of guinea pig ventricular myocytes (cell length 100 μm), the dependence of average dV/dt_{max} on cell-to-cell coupling over the range of normal coupling conductance was very small, but dV/dt_{max} increased with advanced cell-to-cell uncoupling, reflecting the increasing degree of discontinuity.[6,8] A corresponding result was obtained in a study where the degree of coupling was left constant but the cell size was varied in order to modify the degree of discontinuity.[31] This indicates that negligible changes of dV/dt_{max} are expected to occur with moderate changes of cell-to-cell coupling (< 10-fold) in tissue with continuous conduction properties such as synthetic cell strands, an expectation that was confirmed by our simulations (Figure 4A).

In the experimental part of our study, a significantly higher dV/dt_{max} was observed in the HZ than in the WT mice. In the simulations, the data fit to the values in the HZ group (Table 2) was made with the assumption that the sodium inward current, I_{Na}, is the dominant ion charge carrier during the action potential upstroke and implied an upregulation of I_{Na} by 12%. Theoretically, one might argue that voltage clamp experiments would furnish the ultimate proof for a difference in I_{Na}. However, because previous recordings of I_{Na} in single murine myocytes from HZ and WT hearts showed a variability (standard deviations of 22% in HZ and 43% in WT[37]), which exceeded the expected change by almost 2-fold or more, direct recordings of I_{Na} were not repeated. Alternatively, other ion currents might also have caused the small increase in upstroke velocity in HZ animals, and a charge contribution of Ca^{2+} via the L-type Ca^{2+} channel cannot be ruled out.

A further significant change in action potential shape was related to action potential shortening in the HZ versus WT mice. There is no general rule predicting whether a change in cell-to-cell coupling leads to a shortening or a lengthening of the action potential. In tissue with simulated heterogenous distribution of intrinsic action potential duration, cell-to-cell uncoupling canceled the averaging effect of electrotonic interaction, and rendered the local action potentials either longer or shorter according to their intrinsic APD.[38] In a cell chain with a homogenous intrinsic APD, simulation of cell-to-cell uncoupling had no effect on APD (J. Kucera and Y. Rudy, unpublished data, 2003). Thus, the finding of overall APD shortening (Figure 3) in the HZ synthetic strands suggests that remodeling of one or more repolarizing membrane currents has taken place, similar to the finding of a change in a depolarizing current during the action potential upstroke.

Why Are Mice With Reduced Expression of Cx43 Arrhythmogenic?

The lack of detectable changes in propagation velocity in this work on an almost 50% reduction in gap junction expression raises the question about the mechanisms of arrhythmias in mice with null mutations of Cx43. The CKO mice with 95% reduction of Cx43 showed almost normal ventricular function after birth and had died suddenly from arrhythmias only by 8 weeks of age.[22] The HZ mice used in this study showed an increased incidence of arrhythmias during myocardial ischemia.[21] Our experimental and theoretical results suggest that the mere change in θ is unlikely to be the major factor in arrhythmogenesis. Two other potential mechanisms might be envisaged (1) Whereas in linear and continuous tissue θ is relatively insensitive to changes in cell-to-cell coupling, small changes in coupling and intermediate stages of uncoupling can markedly affect formation of unidirectional block at sites of tissue

NIH-PA Author Manuscript

NIH-PA Author Manuscript

NIH-PA Author Manuscript

discontinuities (eg, observed with development of fibrosis).[39,40] (2) As suggested by this study, the change in phenotype after a single, specific null mutation of Cx43 is complex and may involve remodeling of ion channels as well, which might contribute to initiation of arrhythmias in $Cx43^{+/-}$ mice.

Supplementary Material

Refer to Web version on PubMed Central for supplementary material.

Acknowledgements

This work was supported by the Swiss National Science Foundation, the Swiss Heart Foundation, and a Cardiovascular Lipid Research Grant from Parke Davis (Division of Warner Lambert Ltd) and Pfizer/Australia Ltd, NIH grants HL58507 (J.E.S.), HL49054 (Y.R.), and HL333343 (Y.R.) and the Swiss Foundation for Stipends in Biology and Medicine (J.P.K.).

References

1. Saffitz JE, Davis LM, Darrow BJ, Kanter HL, Laing JG, Beyer EC. The molecular basis of anisotropy: role of gap junctions. J Cardiovasc Electrophysiol 1995;6:498–510. [PubMed: 7551319]
2. Burt JM, Massey KD, Minnich BN. Uncoupling of cardiac cells by fatty acids: structure-activity relationships. Am J Physiol 1991;260:C439–C448. [PubMed: 2003571]
3. Rudisuli A, Weingart R. Electrical properties of gap junction channels in guinea-pig ventricular cell pairs revealed by exposure to heptanal. Pflugers Arch 1989;415:12–21. [PubMed: 2482959]
4. Kléber AG, Riegger CB, Janse MJ. Electrical uncoupling and increase of extracellular resistance after induction of ischemia in isolated, arterially perfused rabbit papillary muscle. Circ Res 1987;61:271–279. [PubMed: 3621491]
5. Peters NS, Coromilas J, Severs NJ, Wit AL. Disturbed connexin43 gap junction distribution correlates with the location of reentrant circuits in the epicardial border zone of healing canine infarcts that cause ventricular tachycardia. Circulation 1997;95:988–996. [PubMed: 9054762]
6. Rudy Y, Quan WL. A model study of the effects of the discrete cellular structure on electrical propagation in cardiac tissue. Circ Res 1987;61:815–823. [PubMed: 3677338]
7. Rohr S, Kucera JP, Kleber AG. Slow conduction in cardiac tissue, I: effects of a reduction of excitability versus a reduction of electrical coupling on microconduction. Circ Res 1998;83:781–794. [PubMed: 9776725]
8. Shaw RM, Rudy Y. Ionic mechanisms of propagation in cardiac tissue: roles of the sodium and L-type calcium currents during reduced excitability and decreased gap junction coupling. Circ Res 1997;81:727–741. [PubMed: 9351447]
9. Peters NS, Green CR, Poole-Wilson PA, Severs NJ. Reduced content of connexin43 gap junctions in ventricular myocardium from hypertrophied and ischemic human hearts. Circulation 1993;88:864–875. [PubMed: 8394786]
10. McIntyre H, Fry CH. Abnormal action potential conduction in isolated human hypertrophied left ventricular myocardium. J Cardiovasc Electrophysiol 1997;8:887–894. [PubMed: 9261715]
11. Darrow BJ, Fast VG, Kleber AG, Beyer EC, Saffitz JE. Functional and structural assessment of intercellular communication: increased conduction velocity and enhanced connexin expression in dibutyryl cAMP-treated cultured cardiac myocytes. Circ Res 1996;79:174–183. [PubMed: 8755993]
12. Zhuang J, Yamada KA, Saffitz JE, Kléber AK. Pulsatile stretch remodels cell-to-cell communication in cultured myocytes. Circ Res 2000;87:316–322. [PubMed: 10948066]
13. Saffitz JE, Green KG, Kraft WJ, Schechtman KB, Yamada KA. Effects of diminished expression of connexin43 on gap junction number and size in ventricular myocardium. Am J Physiol Heart Circ Physiol 2000;278:H1662–H1670. [PubMed: 10775147]
14. Reaume AG, de Sousa PA, Kulkarni S, Langille BL, Zhu D, Davies TC, Juneja SC, Kidder GM, Rossant J. Cardiac malformation in neonatal mice lacking connexin43. Science 1995;267:1831–1834. [PubMed: 7892609]

NIH-PA Author Manuscript

NIH-PA Author Manuscript

NIH-PA Author Manuscript

15. Ya J, Erdtsieck-Ernste EB, de Boer PA, van Kempen MJ, Jongsma H, Gros D, Moorman AF, Lamers WH. Heart defects in connexin43-deficient mice. Circ Res 1998;82:360–366. [PubMed: 9486664]
16. Eloff BC, Lerner DL, Yamada KA, Schuessler RB, Saffitz JE, Rosenbaum DS. High resolution optical mapping reveals conduction slowing in connexin43-deficient mice. Cardiovasc Res 2001;51:681–690. [PubMed: 11530101]
17. Guerrero PA, Schuessler RB, Davis LM, Beyer EC, Johnson CM, Yamada KA, Saffitz JE. Slow ventricular conduction in mice heterozygous for a connexin43 null mutation. J Clin Invest 1997;99:1991–1998. [PubMed: 9109444]
18. Morley GE, Vaidya D, Samie FH, Lo C, Delmar M, Jalife J. Characterization of conduction in the ventricles of normal and heterozygous Cx43 knockout mice using optical mapping. J Cardiovasc Electrophysiol 1999;10:1361–1375. [PubMed: 10515561]
19. Thomas SA, Schuessler RB, Berul CI, Beardslee MA, Beyer EC, Mendelsohn ME, Saffitz JE. Disparate effects of deficient expression of connexin43 on atrial and ventricular conduction: evidence for chamber-specific molecular determinants of conduction. Circulation 1998;97:686–691. [PubMed: 9495305]
20. Vaidya D, Tamaddon HS, Lo CW, Taffet SM, Delmar M, Morley GE, Jalife J. Null mutation of connexin43 causes slow propagation of ventricular activation in the late stages of mouse embryonic development. Circ Res 2001;88:1196–1202. [PubMed: 11397787]
21. Lerner DL, Beardslee MA, Saffitz JE. The role of altered intercellular coupling in arrhythmias induced by acute myocardial ischemia. Cardiovasc Res 2001;50:263–269. [PubMed: 11334830]
22. Gutstein DE, Morley GE, Tamaddon H, Vaidya D, Schneider MD, Chen J, Chien KR, Stuhlmann H, Fishman GI. Conduction slowing and sudden arrhythmic death in mice with cardiac-restricted inactivation of con-nexin43. Circ Res 2001;88:333–339. [PubMed: 11179202]
23. Thomas SP, Bircher-Lehmann L, Thomas SA, Zhuang J, Saffitz JE, Kleber AG. Synthetic strands of neonatal mouse cardiac myocytes: structural and electrophysiological properties. Circ Res 2000;87:467–473. [PubMed: 10988238]
24. Rohr S, Scholly DM, Kleber AG. Patterned growth of neonatal rat heart cells in culture: morphological and electrophysiological characterization. Circ Res 1991;68:114–130. [PubMed: 1984856]
25. Fast VG, Kleber AG. Microscopic conduction in cultured strands of neonatal rat heart cells measured with voltage-sensitive dyes. Circ Res 1993;73:914–925. [PubMed: 8403261]
26. Johnson CM, Kanter EM, Green KG, Laing JG, Betsuyaku T, Beyer EC, Steinberg TH, Saffitz JE, Yamada KA. Redistribution of connexin45 in gap junctions of connexin43-deficient hearts. Cardiovasc Res 2002;53:921–935. [PubMed: 11922902]
27. Saffitz JE, Kanter HL, Green KG, Tolley TK, Beyer EC. Tissue-specific determinants of anisotropic conduction velocity in canine atrial and ventricular myocardium. Circ Res 1994;74:1065–1070. [PubMed: 8187276]
28. Luo CH, Rudy Y. A dynamic model of the cardiac ventricular action potential, I: simulations of ionic currents and concentration changes. Circ Res 1994;74:1071–1096. [PubMed: 7514509]
29. Faber GM, Rudy Y. Action potential and contractility changes in $[Na^+]_i$ overloaded cardiac myocytes: a simulation study. Biophys J 2000;78:2392–2404. [PubMed: 10777735]
30. Kleber AG, Riegger CB. Electrical constants of arterially perfused rabbit papillary muscle. J Physiol 1987;385:307–324. [PubMed: 3656162]
31. Spach MS, Heidlage JF, Dolber PC, Barr RC. Electrophysiological effects of remodeling cardiac gap junctions and cell size: experimental and model studies of normal cardiac growth. Circ Res 2000;86:302–311. [PubMed: 10679482]
32. Fast VG, Darrow BJ, Saffitz JE, Kleber AG. Anisotropic activation spread in heart cell monolayers assessed by high-resolution optical mapping: role of tissue discontinuities. Circ Res 1996;79:115–127. [PubMed: 8925559]
33. Gourdie RG, Green CR, Severs NJ. Gap junction distribution in adult mammalian myocardium revealed by an anti-peptide antibody and laser scanning confocal microscopy. J Cell Sci 1991;99:41–55. [PubMed: 1661743]
34. Wikswo, JP. Tissue anisotropy, the cardiac biodomain, and the virtual electrode effect. In: Zipes, DP.; Jalife, J., editors. Cardiac Electrophysiology: From Cell to Bedside. Philadelphia, Pa: Saunders; 1995. p. 348-361.

NIH-PA Author Manuscript

NIH-PA Author Manuscript

NIH-PA Author Manuscript

35. Knisley SB, Hill BC. Effects of bipolar point and line stimulation in anisotropic rabbit epicardium: assessment of the critical radius of curvature for longitudinal block. IEEE Trans Biomed Eng 1995;42:957–966. [PubMed: 8582725]

36. Pimentel RC, Yamada KA, Kleber AG, Saffitz JE. Autocrine regulation of myocyte Cx43 expression by VEGF. Circ Res 2002;90:671–677. [PubMed: 11934834]

37. Johnson CM, Green KG, Kanter EM, Bou-Abboud E, Saffitz JE, Yamada KA. Voltage-gated Na^+ channel activity and connexin expression in Cx43-deficient cardiac myocytes. J Cardiovasc Electrophysiol 1999;10:1390–1401. [PubMed: 10515564]

38. Viswanathan PC, Shaw RM, Rudy Y. Effects of I_{Kr} and I_{Ks} heterogeneity on action potential duration and its rate dependence: a simulation study. Circulation 1999;99:2466–2474. [PubMed: 10318671]

39. Fast VG, Kleber AG. Block of impulse propagation at an abrupt tissue expansion: evaluation of the critical strand diameter in 2- and 3-dimensional computer models. Cardiovasc Res 1995;30:449–459. [PubMed: 7585837]

40. Rohr S, Kucera JP, Fast VG, Kleber AG. Paradoxical improvement of impulse conduction in cardiac tissue by partial cellular uncoupling. Science 1997;275:841–844. [PubMed: 9012353]

NIH-PA Author Manuscript

NIH-PA Author Manuscript

NIH-PA Author Manuscript

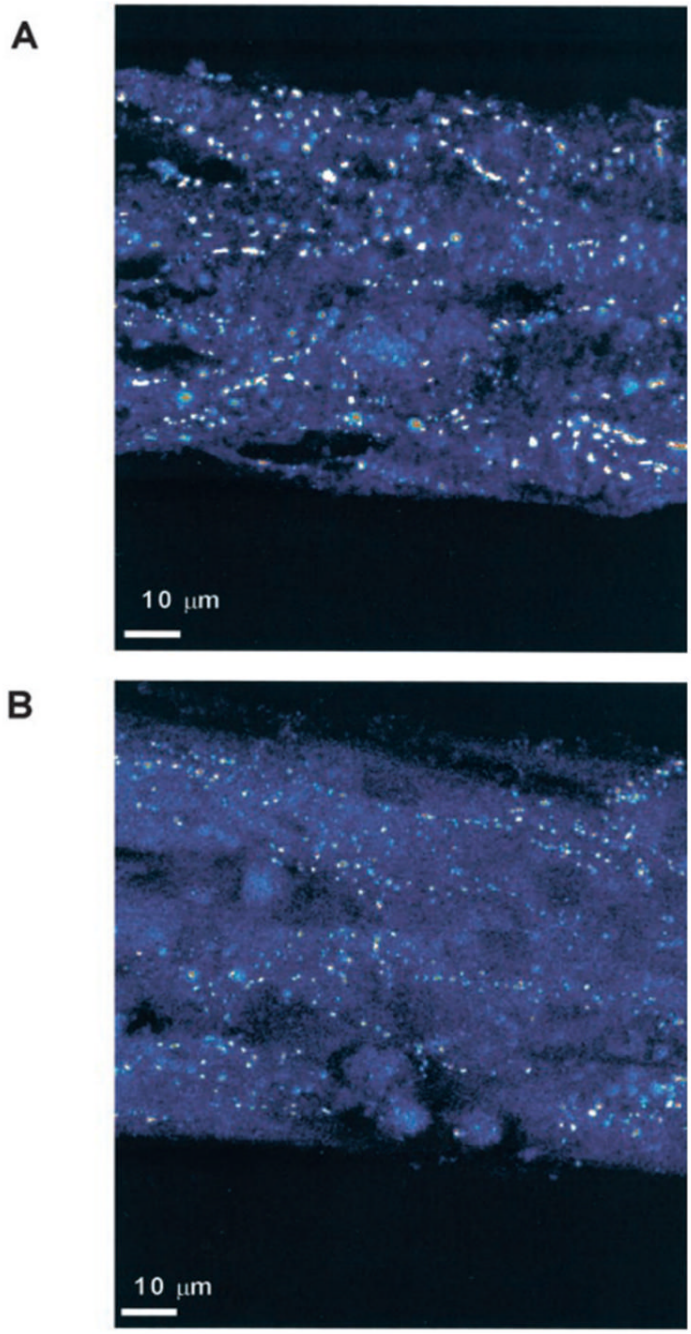

Figure 1.
Immunofluorescent staining of connexin43 in synthetic strands of neonatal murine ventricular myocytes composed of WT and HZ myocytes. Lower density of gap junctions in B corresponds to an average reduction of 43% in HZ vs WT strands (see also Table 1).

NIH-PA Author Manuscript

NIH-PA Author Manuscript

NIH-PA Author Manuscript

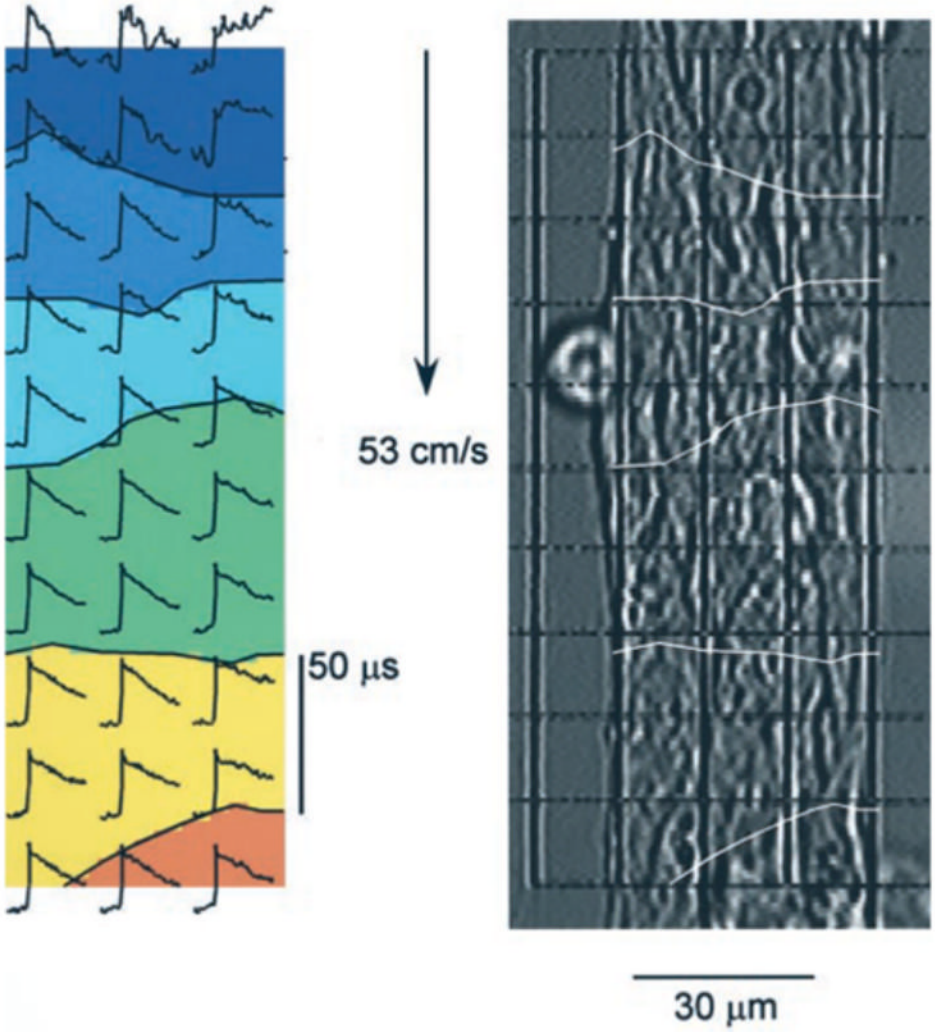

Figure 2.

Electrical impulse propagation in synthetic strands of HZ neonatal murine myocytes assessed with optical mapping. Right, Microscopic picture of a synthetic murine myocyte strand with superimposed grid indicating size and position of measuring diodes (15 μm × 15 μm). Picture allows for delineation of cell borders. Left, Isochrone map of electrical impulse propagation from top to bottom; the area between the isochrone lines denotes an interval of 50 μs. Initial portions of individual action potentials are shown for each diode location. Conduction velocity is 53 cm/s.

NIH-PA Author Manuscript

NIH-PA Author Manuscript

NIH-PA Author Manuscript

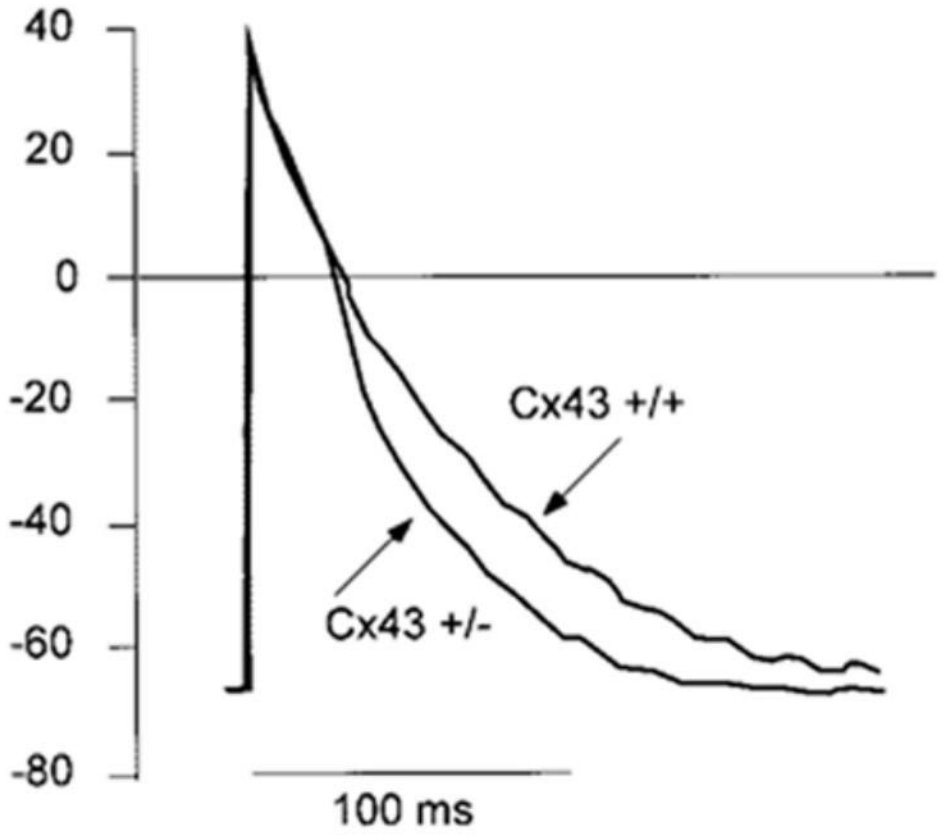

Figure 3.
Microelectrode recordings of transmembrane action potentials from cells within the synthetic strands in WT and HZ mice. Action potentials are identical at this recording speed with exception of the repolarization phase that is significantly shorter in HZ mice at APD90 (see also Table 2).

NIH-PA Author Manuscript
NIH-PA Author Manuscript
NIH-PA Author Manuscript

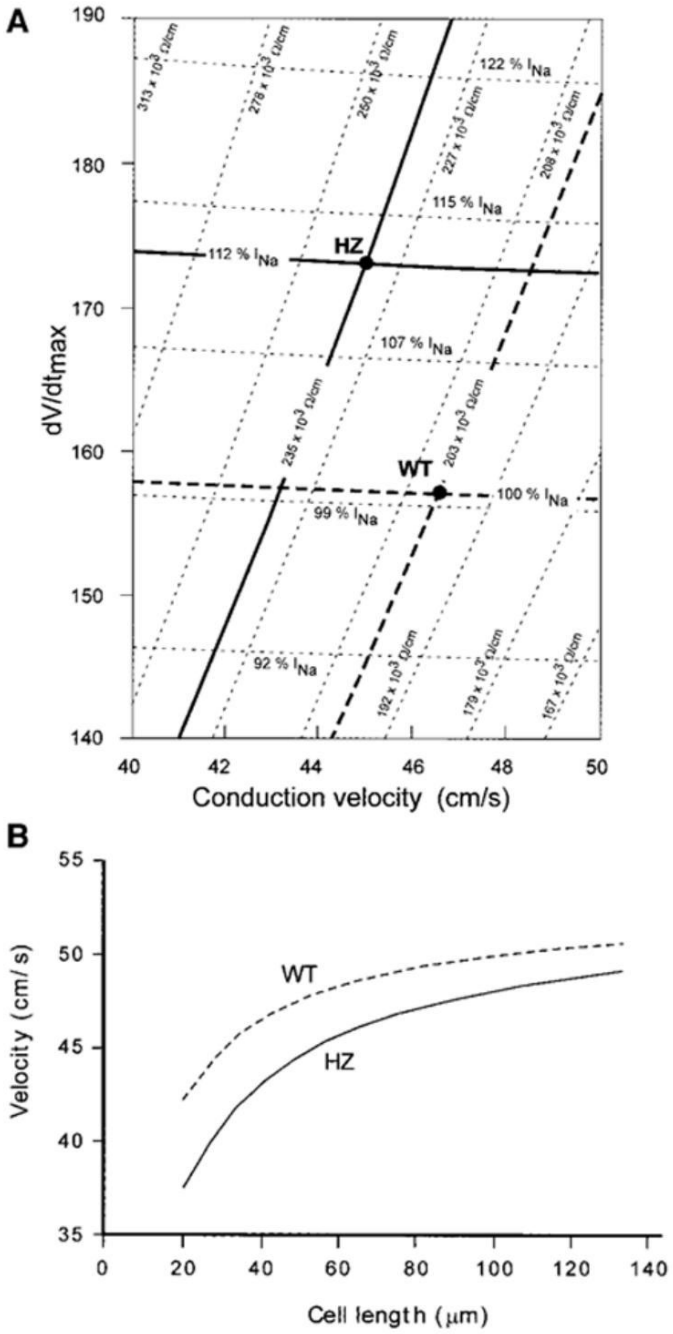

Figure 4.

A, Simulation of the relationship between dV/dt_{max} of the action potential upstroke and conduction velocity in a myocyte strand having a cell length of 40 μm. Bold dashed lines cross at a point in the "dV/dt_{max} velocity phase space" that corresponds to the experimental data in the WT strands. Simulating conduction without changing I_{Na}, but with a 43% reduction of Cx43 expression yields an almost unchanged dV/dt_{max}, at a velocity of 43.2 cm/s (crossing of the bold horizontal dotted line with the oblique bold solid line). A fit to the experimentally determined HZ values (crossing of the bold solid lines) is only possible by an upregulation of I_{Na} by 12%. B, Simulation of the effect of cell length, l, on conduction velocity, θ, in WT murine synthetic strands (top curve) and HZ strands (bottom curve). Simulation was initiated

from the fit to the experimental data at $l = 40\ \mu$ m. Note that increasing l has two effects: it increases θ and it reduces the effects of a difference in Cx43 expression between WT and HZ.

NIH-PA Author Manuscript
NIH-PA Author Manuscript
NIH-PA Author Manuscript

NIH-PA Author Manuscript NIH-PA Author Manuscript NIH-PA Author Manuscript

TABLE 1

Quantitative Immunofluorescence of Cx43 in Synthetic Strands of $Cx43^{+/-}$ (HZ) Versus $Cx43^{+/+}$ (WT) Mice

Genotype	Strand Width, μm	No. of Cultures	Gap Junction Fluorescence, % cell area	No. of Gap Junctions, per 100 μm^2	Relative Gap Junction Size, μm^2
HZ	100	5	0.86 ± 0.37	1.90 ± 0.63	0.45 ± 0.10
HZ	80	5	0.70 ± 0.23	1.83 ± 0.46	0.38 ± 0.11
HZ	60	5	0.82 ± 0.21	1.88 ± 0.48	0.45 ± 0.11
			0.79 ± 0.08 *†	1.87 ± 0.04 *†	0.43 ± 0.04 †
WT	100	5	1.27 ± 0.43	2.52 ± 0.58	0.49 ± 0.11
WT	80	7	1.44 ± 0.33	2.71 ± 0.70	0.54 ± 0.11
WT	60	5	1.29 ± 0.32	2.33 ± 0.77	0.54 ± 0.10
			1.33 ± 0.09 *‡	2.52 ± 0.19 *‡	0.52 ± 0.03 ‡

HZ vs WT,

* $P < 0.001$. All data are mean ± SD.

† Mean values $Cx43^{+/-}$.

‡ Mean values $Cx43^{+/+}$.

NIH-PA Author Manuscript NIH-PA Author Manuscript NIH-PA Author Manuscript

TABLE 2

Electrical Properties of Synthetic Cardiomyocyte Strands: $Cx43^{+/-}$(HZ) Versus $Cx43^{-/-}$(WT) Mice

Microelectrode Data	**n**	**MDP, mV**	**APA, mV**	**dV/dt_{max}, V/s**	**APD_{50}, ms**	**APD_{90}, ms**
Genotype						
HZ	4	69 ± 8	102 ± 9	183 ± 64	29 ± 13	90 ± 12
WT	8	68 ± 6	101 ± 7	161 ± 44	37 ± 20	111 ± 20
P	NS	NS	NS	NS	NS	0.04
Optical Data	n	θ, cm/s	dV/dt_{max}, % APA/s			
Genotype						
HZ	104	45.0 ± 12	173 ± 28			
WT	79	46.6 ± 13	157 ± 27			
P		NS	0.0005			

MDP indicates maximal diastolic potential; APA, action potential amplitude; APD, action potential duration; and dV/dt_{max}, maximal upstroke velocity of the transmembrane action potential in V/s (electrical recordings) or percent action potential amplitude/s (optical recordings). 1% APA/s corresponds to 1 V/s at an APA of 100 mV. θ indicates propagation velocity in cm/s.

P values related to difference between WT and HZ. All data are mean ± SD. NS indicates not significant.